Universiteit Antwerpen

This item is the archived peer-reviewed author-version of:

Theoretical investigation of electronic, vibrational, and nonlinear optical properties of 4-fluoro-4-hydroxybenzophenone

Reference:
Pegu David, Deb Jyotirmoy, Van Alsenoy Christian, Sarkar Utpal.- Theoretical investigation of electronic, vibrational, and nonlinear optical properties of 4-fluoro-4-hydroxybenzophenone
Spectroscopy letters - ISSN 0038-7010 - 50:4(2017), p. 232-243
Full text (Publisher's DOI): https://doi.org/10.1080/00387010.2017.1308381
To cite this reference: http://hdl.handle.net/10067/1432330151162165141

uantwerpen.be
Institutional repository IRUA

Theoretical Investigation of Electronic, Vibrational and Nonlinear Optical Properties of 4-fluoro-4-hydroxybenzophenone

David Pegu[1], Jyotirmoy Deb[1], Christian Van Alsenoy[2], Utpal Sarkar[1]

[1]Department of Physics, Assam University, Silchar, Assam, India
[2]Department of Chemistry, University of Antwerp, Groenenborgerlaan, Antwerpen, Belgium

Corresponding to author: Utpal Sarkar . Email: utpalchemiitkgp@yahoo.com

Abstract

The present study emphasizes on structural, opto-electronic, vibrational and non-linear properties, at electronic structure level, on 4-fluoro-4-hydoxybenzophenone molecule using the first principle calculation. Detailed vibrational assignments of the wavenumbers are carried out on the basis of potential energy distribution and a good agreement between the reported and calculated wavenumber has been observed. Further, molecular electrostatic potential surface predicts the reactive site of the molecule. From the time dependent density functional theory analysis on UV-visible spectra, a red shift has been observed on maximum absorption wavelength when gaseous medium is replaced by solvent medium. The nonlinear optical property of the 4-fluoro-4-hydroxybenzophenone molecule shows that this molecule possesses large nonlinear optical properties which might make it useful for various nonlinear optical applications.

KEYWORDS: 4-fluoro-4-hydroxybenzophenone; density functional theory; chemical reactivity; nonlinear optical properties; vibrational spectroscopy

Accepted Manuscript

INTRODUCTION

In 1865 the structural studies of Benzophenone were done by Linneman [1] after the successful synthesis of this material. The stable orthorhombic phase and melting point (48 - 48.5 ^{0}C) of the Benzophenone molecule was also reported by Linneman. Benzophenone and its derivatives have gained significant attraction to the researchers in present days due to their enormous application in various fields. Investigations on the structure of benzophenone molecule have been a subject of great interest because of the existence of polymorphism on this molecule and its transformation from metastable phase to stable phase [2]. The stable phase benzophenone molecule is found to be a promising material for crystal-growth experiments [2]. Another fascinating characteristic of the benzophenone molecule is that it exhibits large Raman shifts of more than 3000 cm^{-1} and can be regarded as a suitable candidate for Raman laser application [3]. Benzophenone molecule and its derivatives are widely used for the purpose of blocking of ultraviolet (UV) radiation and in sunscreen products because of their ability to absorb UV rays in great extent [4]. It is also used in some major industrial applications such as in manufacture of insecticides [5], in cosmetic products [6], anticancer agent [6], anti-aging products [6], additive for plastics and coatings [7]. These molecules also found their importance in biological applications as photo-physical probes in order to identify the map-protein interaction [8-9]. Further, due to non-centrosymmetric structure, benzophenone molecule may be used for the fabrication of nonlinear optical materials [10-17].

A large number of investigations have been performed recently in order to study structural, electronic, polarization characteristics and vibrational spectra of benzophenone

Accepted Manuscript

derivatives [2-4, 18-19]. Vibrational modes of benzophenone/substituted benzophenones have also been discussed by various researchers in different phases such as vapor, liquid and crystals [20-23]. Several spectroscopic, polarization absorption properties and UV electronic transition studies of halogen and methyl substituted benzophenone have been reported in the literature [24-28] from time to time. The introduction of a substituent group in benzene rings results a change in charge distribution of the molecule and consequently influence various properties such as structural, electronic and vibrational assignments [19]. Elements like F, Cl, and O have large electronegativity value as a consequence of which they show high electron withdrawing capability. When these elements are used as substituent in aromatic molecules chemical reactivity profile, as well as excitation energies of aromatic molecule and its substituted one, differ with each other [19]. Computational methods are widely used for interpreting and assigning experimental infrared or Raman spectra [29-30]. A combinations of various theoretical calculations such as infrared (IR), Raman and UV–Vis spectra provides valuable structural information of the system concerned.

In the present work, substitution in the benzophenone molecule has been done by introducing fluorine atom and hydroxyl group. Theoretical investigations have been carried out on 4-fluoro-4-hydroxybenzophenone molecule (4F4OHBP) to observe the extent of influence of substitution on the structural parameters (bond length, bond angle and dihedral angle), electronic properties (molecular orbital energies, energy gap), chemical reactivity profile (chemical potential, chemical hardness, electrophilicity index) and nonlinear optical properties (dipole moment, polarizability and hyperpolarizability).

Accepted Manuscript

Theoretical UV-visible spectroscopic analysis and vibrational analysis of the 4F4OHBP molecule have been performed. The vibrational assignment of the molecule under study is compared with the previous theoretical findings. A comparison is also made between theoretically predicted Infrared (IR) and Raman spectra with that of available experimental data taken from SDBS database [31].

COMPUTATIONAL METHODS

The geometry optimization of the molecule has been achieved by using HF and DFT schemes. All calculations have been performed using Gaussian 09 package. Various functionals such as B3LYP, B3PW91, CAM-B3LYP and 6-311++G(d,p) as basis set [32] have been used for the calculation. The TD-DFT and frequency calculations have also been carried out using the same level of theory as that of geometry optimization and the absence of imaginary frequency confirms the minimum potential energy surface of the structure. The visual presentation of the vibrational assignments of the computed wavenumbers is achieved using animation option of GAUSSVIEW program [33]. The potential energy distributions (PED) of normal modes are determined using GAR2PED software package [34].

The global reactivity parameters such as chemical potential [35], chemical hardness (η) [36], and electrophilicity index (ω) [37-38] are calculated using the given relations;

$$\mu = -\frac{I + A}{2}$$

$$\eta = I - A$$

Accepted Manuscript

$$\omega = \frac{\mu^2}{2\,\eta}$$

$$I = -E_{HOMO}$$

$$A = -E_{LUMO}$$

where I and A are the ionization energy and electron affinity respectively.

IR intensities (I_i) and Raman activities (S_i) are calculated using B3LYP, B3PW91 and CAM-B3LYP functionals. The Raman activity can be converted to Raman intensity (R_i) using the relation obtained from the basic principle of Raman scattering [39]

$$R_i = \frac{f\ (\nu_0 - \nu_i)^4\ S_i}{\nu_i \left(1 - e^{\left(-\frac{hc\nu_i}{KT}\right)}\right)}$$

where ν_0 is the frequency of the incident radiation for excitation, ν_i is the wavenumber of vibrational modes, h, c, k are the universal constants and f is the normalization factor for all the intensities.

RESULTS AND DISCUSSION

Structural Properties

The total energy with zero-point vibrational energy correction of the compound using HF, B3LYP, B3PW91 and CAM-B3LYP functional are -746.882, -751.300, -750.999, -750.944 Hartree respectively.

Among the four methods, B3LYP functional shows lowest energy compare to other three functionals considered here. The optimized geometry of the molecule with atom

Accepted Manuscript

numbering scheme is shown in Fig. 1. The bond lengths between various C-C bonds within the benzene ring are not equal. The bond lengths C1-C2, C6-C1, C14-C15, C14-C19 in the benzene ring appears to be a little larger and the bond lengths C3-C4, C4-C5, C15-C16, and C18-C19 are shorter than the regular hexagonal symmetry of the benzene ring. The deviation of the regular hexagonal symmetry of the benzene ring is also obvious from the decrease in values of the bond angles C2-C3-C4, C4-C5-C6, C14-C15-C16 and increase in C3-C4-C5, C1-C2-C3, C5-C6-C1 and C16-C17-C18. With the substitution of fluorine and hydroxyl group on the carbon atoms of the benzene rings, the variation of bond lengths and bond angles in the benzene rings takes place and this is attributed to the change in charge distribution of the carbon atoms of the benzene rings. It is observed that various bond distances and bond angles of the compound are nearly found to be same at B3LYP and B3PW91 level of theory but the magnitude is slightly higher in case of B3LYP method. Also the values obtained using these two methods are close to the experimental ones. The structural parameters such as bond lengths, bond angles and dihedral angles between different atoms of 4F4OHBP molecule are tabulated in Table 1 and the results obtained are compared with the available experimental values of the same type of compounds, namely, benzophenone [23] and 4,4-dimethylbenzophenone [40]. On comparing the theoretical and experimental results of the present study, it is observed that the theoretical results are slightly overestimated. This may be due to the fact that the experimental and theoretical values are for two similar but essentially different molecules, besides the difference of isolated gas phase structure [41-42] and condensed phases. It has been noticed that the dihedral angle between the two benzene rings (C6-C1-C14-C19) in gas phase is found to be 51.91^0

Accepted Manuscript

which is in close agreement with its normal value of 54.00^0 for the unsubstituted benzophenone [43]. But in solvent phase, the dihedral angle value slightly increases compare to that in the gas phase (Table 2).

The C-H bond length in pure benzophenone is 1.08 Å but the (C-F) bond length is found to be 1.35 Å when H atom is replaced by F atom. The dihedral angle between two benzene rings slightly decreases in case of fluorine substituted benzophenone structure (53.27^0) compare to unsubstituted one. The introduction of hydroxyl group into pure benzophenone structure increases the bond length to 1.36 Å and it also decreases the dihedral angle between two benzene rings to 52.35^0 compare to pure benzophenone. The bond angle between carbons atoms (C3-C4-C5) in the phenyl ring I of fluorine substituted benzophenone is higher than the normal value (120.00^0) and it is due to the electron withdrawing nature of the fluorine atom. However, the bond angle (C16-C17-C18) in the phenyl ring II is not so much affected by the substitution of hydroxyl group.

Electronic Properties

Highest occupied molecular orbital (HOMO) and lowest unoccupied molecular orbital (LUMO) are considered to be very essential parameters to study the electrical and optical properties of molecule. The energy gap (E_{LUMO}-E_{HOMO}) is an important stability index which helps to characterize the chemical reactivity and stability of the molecule [44] via maximum hardness principle (MHP) [45]. The spectroscopic properties of a system strongly depend on the energy gap of the system. The lower value of energy gap clearly explains the intramolecular charge transfer interactions taking place within the molecule,

Accepted Manuscript

which affects the bioactivity of the molecule [46]. A molecule with high energy gap is termed as hard molecule and is difficult to polarize because it needs more energy for excitation whereas a molecule with a low energy gap is easy to polarize and relatively more reactive than chemically hard ones as it can easily offer electrons to an acceptor [47]. The calculated ground state energy gap of the molecule is 4.717 eV (Table 3), using B3LYP/6-311++G(d,p) method, showing minimum energy gap among all the functionals. The chemical reactivity descriptors play a significant role to study the reaction pathway [48], some excited state phenomena [49-52] and also used as an effective tool for toxicity analysis [53-54]. The chemical reactivity parameters of the molecule are presented in Table 3. The reactivity parameters include ionization potential, electron affinity, chemical hardness, chemical potential, and electrophilicity index which are described here in terms of molecular orbital theory. The chemical hardness of pure benzophenone molecule is found to be 4.904 eV (Table S1) and the value decreases to 4.717 eV due to the substitution of fluorine atom and hydroxyl group. The smaller value of chemical hardness in case of substituted benzophenone indicates that the chemical stability of the system decreases and thus the system becomes more reactive. The 4-fluoro-4-hydroxybenzophenone molecule possess higher polarizability compare to its pure counterpart which correlates the maximum hardness principle (MHP) [45] with the minimum polarizability principle (MPP) [55]. A number of theoretical studies reveal that electrophilicity is a reliable reactivity descriptor of quantum chemistry [56-57] and it is also a good indicator of stabilization energy [58]. Parr *et al.* defined [38] electrophilicity index as the measure of energy lowering associated with the maximum amount of electron flow between two species and therefore, represents the collective electrophilic

Accepted Manuscript

nature of a molecule. However, as per the Koopmans' theorem [59] E_{LUMO} is related to the electron affinity (A) of a molecule and, as such, characterizes the susceptibility of a molecule for attack by nucleophiles. Though, the elctrophilicity index (ω) and electron affinity (A) are not actually same, but are strongly correlated quantities, as both of these quantities measure the propensity of electron intake [60]. In case of electrophilcity, fractional amount of electron transfer is possible but in case of electron affinity only one single electron transfer occurs. The electrophilicity of the substituted benzophenone increases significantly compare to pure benzophenone which again confirms the decrease in chemical stability in accordance with the minimum electrophilicity principle (MEP) [61]. As 4-fluoro-4-hydroxybenzophenone molecule is less stable than unsubstituted benzophenone it will show higher tendency to accumulate additional electronic charges from the surroundings. From the Table 3**,** it has been noticed that among the considered functionals, the highest value of electrophilicity index of the 4F4OHBP molecule is obtained using B3LYP functional with a magnitude of 2.071 eV. The chemical potential (μ) is generally defined as the negative of electronegativity (χ) and it describes the tendency of gaining electrons towards the molecule. Electrons generally flow from low electronegativity to high electronegativity region until the electronegativity value of the constituent system neutralizes. The magnitude of chemical potential for 4F4OHBP molecule is -4.421 eV when determined using B3LYP functional.

Some important molecular orbitals (i.e. HOMO-1, HOMO, LUMO, and LUMO+1) of the 4F4OHBP molecule have been described here, as shown in Fig. 2. The molecular orbital figures reflect that HOMO is mainly localized over the O atom of the carbonyl group,

Accepted Manuscript

phenyl ring (phII) and the hydroxyl group connected to phII. On the other hand, LUMO is almost spread over the entire molecule except the H atom attached to the hydroxyl group and some of the H atoms of the phenyl rings (phI and phII). However, in case of HOMO-1, electrons are localized mainly over phenyl ring (phI) connected to fluorine atom, some part of the phenyl ring (phII) attached to the hydroxyl group, O atom of the hydroxyl group and carbonyl group, while in LUMO+1 electrons are found to be localized almost over entire molecule except for hydroxyl group, carbonyl group and F atom.

Molecular Electrostatic Potential

Electrostatic potential (ESP), electron density (ED) and molecular electrostatic potential (MEP) surface are plotted, as shown in Fig. 3 to predict the possible reactive sites for electrophilic and nucleophilic attack of the investigated molecule, which is a useful tool for investigating the reactivity profile of the molecular species. The ED plot of the studied molecule shows a uniform electron distribution. From the ESP plot (Fig. 3 (b)) it has been noticed that the localization of negative ESP dominates over the entire molecule and it is also obvious as there is a correlation between ESP and electronegativity. In the MEP plot blue color represents the maximum positive region where the nucleophilic attack takes place whereas the yellow region represents the site of electrophilic attack with the maximum negative region. In our studied molecule, it has been found that the most electrophilic region is near the O13 atom which is the dark yellow region in the MEP plot (Fig. 3 (a)) whereas the yellowish color near the O25 and F9 atoms represent the region of less electrophilicity of the molecule as compared to O13 atom. The

Accepted Manuscript

hydrogen atom (H22) attached to the hydroxyl group corresponds to the most positive region of the molecule which is the blue colored region. Herein lies the importance of MEP that it simultaneously displays not only molecular size, shape but also shows the electrostatic potential regions (positive, negative and neutral regions) of the molecule under analysis. Different types of colors are used to represent different values of electrostatic potential at the surface of the molecule and the potential increases following the trend, red < orange < yellow < green < blue. The ESP figure also confirms that the negative regions were found around O13 atom of the C=O group.

Nonlinear Optical Properties

In recent years search of new type of material showing efficient nonlinear optical properties became an emerging topic to the researchers. Nonlinear optical materials are vastly used in optical data storage, optical communication, optical switching, optical modulators and in signal processing technology [62-64]. Dipole moment, polarizability and hyperpolarizability etc. are important optical response properties of organic molecule. Since NLO properties are structure-sensitive, NLO properties may be studied [65] to get insight of the molecular structure. There has been numerous investigation for molecules with large hyperpolarizabilities (β) which arise due to the intermolecular charge transfer of the π-conjugated electron cloud from an electron donor to electron acceptor group. In our present study, the electric dipole moment, molecular polarizability, anisotropy of polarizability and first hyperpolarizability of 4F4OHBP molecule are studied.

Accepted Manuscript

The higher magnitude of dipole moment, polarizability, and first hyperpolarizability are important factors of a molecule for designing a material which exhibits better NLO performance. The dipole moment, polarizability, and first hyperpolarizability values are presented in Table 4. The dipole moment, polarizability, and first order hyperpolarizability values calculated using B3LYP functional are found to be 1.171 Debye, 1.403×10^{-30} e.s.u., and 7.226×10^{-30} e.s.u. respectively. The magnitude of the Z-component of the dipole moment is found to be highest with the value 1.127 Debye and it was expected due to the orientation of the molecule, while it is lowest along X-direction (0.076 Debye). The molecular polarizability computed with B3LYP functional of the molecule is mainly attributed due to α_{zz} component of polarizability. Using the same functional, it is found that longitudinal component β_{zzz} mainly contributes to the first hyperpolarizability of the molecule, which reflects that considerable delocalization of charge has taken place along the given direction. Urea is generally used as a reference molecule for comparative study of nonlinear optical properties. The values of dipole moment, polarizability and first order hyperpolarizability of urea is recorded to be 1.373 Debye, 3.735×10^{-31} e.s.u., and 0.337×10^{-30} e.s.u. respectively. In the present work, it is noticed that the calculated dipole moment of the molecule under study is nearly same as that of urea whereas polarizability and first order hyperpolarizability are 3.76 and 21.4 times greater than that of urea, as obtained using B3LYP functional with 6-311++G(d,p) basis set. The large value of hyperpolarizability of the 4F4OHBP molecule ensures that this molecule may be recommended for future nonlinear optical applications.

Optical Property (Uv-Visible Absorption Spectra)

Accepted Manuscript

The UV spectroscopy is used to understand the nature of electronic structure and various electronic excited states of the molecules and also to check whether the compound is showing NLO properties or not. The calculated excitation energies (E), oscillator strengths (f), wavelengths (λ) and their major contribution for the transitions are shown in Table 5. The UV-Visible spectra in gas and solvent phase of 4F4OHBP molecule are shown in Fig. 4. The TD-DFT calculation reveals that intense electronic transition is observed in gas phase at wavelength 286.6 nm (Fig. 4(a)) having oscillator strength 0.287 with the corresponding electronic transitions from HOMO→LUMO (60%) and HOMO-1→LUMO (28%). In case of dimethyl sulfoxide (DMSO), electronic transition is observed at wavelength 302.4 nm (Fig. 4(b)) with oscillator strength 0.388 and significant absorption peak is observed due to the electronic transitions HOMO→LUMO (66%) and HOMO-1→LUMO (20%). However, when chloroform and ethanol are used as solvent, electronic transitions are observed at wavelength 298.9 nm (Fig. 4(c)) and 301.2 nm (Fig. 4(d)) having oscillator strength 0.387 and 0.368 and the related electronic transitions are HOMO→LUMO (68%), HOMO-1→LUMO (20%) and HOMO-1→LUMO (19%), HOMO→LUMO (67%) respectively. These electronic absorption corresponds to the transition from ground state to first excited state and is mainly described by one electron excitation from the highest occupied molecular orbital (HOMO) to the lowest unoccupied molecular orbital (LUMO). It has been observed that the wavelength associated with the intense absorption peak increases as we move from gas phase to solvent phase which indicates the occurrence of red shift of highest peak in absorption spectra. With increase of solvent polarity, the absorption wavelength shifted

Accepted Manuscript

towards higher wavelength side i.e. red shifted. The probable source of red shift of absorption wavelength in the selected solvents is may be due to solvent polarity.

Vibrational Analysis

A detailed study of fundamental modes of vibration of 4F4OHBP molecule has been done. According to the theoretical calculation, 4-fluoro-4-hydroxybenzophenone molecule has C_1 point group symmetry. The molecule has 25 atoms which provide 69 fundamental modes. The simulated vibrational frequencies have been compared with FT-IR and FT-Raman frequencies obtained from SDBS web site [31]. A comparison is made between the vibrational frequencies calculated using different functionals with the experimental one and the result reveals that the theoretical frequencies are slightly higher than the experimental ones for most of the vibrational modes. This is happening due to the neglect of anharmonic terms and also due to combined effect of electron correlation with the basis set deficiencies. In order to make a good agreement with the experimental frequencies, it is mandatory to scale down the calculated harmonic frequencies as a result of which root mean square deviation between the actual and theoretical result is minimized. The scaling factors used for scaling down the unscaled frequencies are 0.905, 0.961, 0.957, and 0.980 for HF, B3LYP, B3PW91, and CAM-B3LYP functionals respectively [41, 66-67]. The experimental FT-IR and FT-Raman frequency, theoretical vibrational frequency computed with HF, B3LYP, B3PW91, and CAM-B3LYP functionals, along with percentage of potential energy distribution (PED) is provided in Table 6. The significant vibrational assignments and PED of the studied molecule obtained using B3LYP functional and 6-311++G(d,p) basis set are described here. The

Accepted Manuscript

normal mode vibrations are usually well explained by the PED which is measured as the relative contribution of each displacement coordinate with respect to the total change in the potential energy during the normal vibration [68]. The PED method is also used for determining the combination of various modes present together in a normal vibration but the most significant mode is that which contributes to the maximum PED [19].

In case of aromatic compounds, carbon–hydrogen (C-H) stretching vibrations normally occur at 3000–3100 cm^{-1} [41, 69]. In case of our molecule, the high intensity C-H stretching vibrations are observed in the frequency range 3032 to 3082 cm^{-1}. The asymmetric stretching vibrations are observed at the wavenumbers lying between 3032 and 3070 cm^{-1} and also at 3080 cm^{-1} whereas symmetric stretching modes are observed at the wavenumbers of 3074, 3077 and 3082 cm^{-1}. These stretching vibrations contribute near about 96% of the potential energy distribution (PED). Among the calculated modes, some of the C-H stretching modes are in good agreement with the experimental results of the examined species (Table 6). Literature data reveals that in-plane C-H bending generally occurs in the range 1000-1520 cm^{-1} for the substituted benzenes, whereas the out-of- plane bending falls between 700-1000 cm^{-1} [19, 70]. From our results the C-H in-plane bending vibrations are identified at 1077, 1085, 1130, 1145, 1149, 1196, 1270, 1282, 1315, 1379, 1403, 1472, 1479, 1573 cm^{-1} and the C-H out-of-plane bending vibrations fall at 791, 793, 801, 822, 837, 933, 934, 947, 952 cm^{-1}. These assigned vibrations determined theoretically matches well with the previous results [19, 70] except some in-plane C-H modes which are shifted towards higher frequency range. This shift may probably occur due to the presence of high electronegative elements (F and O)

Accepted Manuscript

connected to the phenyl ring (phI and phII). The highest PED is obtained at wavenumber 1270 cm^{-1} (84%) in case of in-plane bending whereas out-of-plane vibrations have PED of 95%, found at wavenumber 801 cm^{-1}.

The carbonyl stretching vibrations are usually expected in the frequency region 1660-1740 cm^{-1} in case of benzophenone [19]. The sharp intense C=O stretching vibration in the Raman spectrum is occurring at 1650 cm^{-1} for benzophenone [23]. The experimentally reported values of our studied molecule reflect a very strong band at 1637 cm^{-1} in the FT-IR spectroscopy and at 1631 cm^{-1} in the case of FT-Raman spectroscopy, which are assigned as C=O stretching vibration. In present case, a strong intense C=O stretching vibration corresponding to a frequency of 1639 cm^{-1} has been noticed and found that 73% of PED is contributed by this stretching vibration. The theoretically calculated frequency is slightly more than the experimentally observed value of C=O vibration. The reason of this underestimation may be due to the conjugation of C=O bond with the aromatic ring which may increase its single bond character, resulting in a lower value of carbonyl stretching wave numbers [71]. The frequency associated with the C=O in-plane bending vibrations determined theoretically are found to be at 355, 566 and 905 cm^{-1} and that of out-of-plane vibrations at 752 cm^{-1}. The majority of the assigned C=O in-plane and out-of-plane vibrations are in good agreement with the experiment as well as with the literature data [19, 24]. The highest PED contributed by C=O in-plane vibrations is around 23%, whereas 19% of the PED is attributed by out-of-plane C=O vibrations.

Accepted Manuscript

The C-F stretching vibrations for fluoro-benzenes are usually found in FT-IR spectra and it appears in the range 1000-1300 cm^{-1} [72-73]. For the studied molecule, the C-F stretching vibration is observed at 791 and 1196 cm^{-1}. The C-F in-plane bending vibration modes for the mono-fluorinated benzene are normally observed at 250-350 cm^{-1}[74]. The frequency ranges of out-of-plane C-X (X=Cl, F, Br) vibrations of substituted benzene falls between 140-350 cm^{-1} [70]. For the molecule considered in this work, the C-F in-plane bending modes are noticed in the wavenumber range 302-402 cm^{-1}, while the out-of-plane vibrations are obtained at wavenumbers 148, 193, 483, 537 cm^{-1}. But except the vibration observed at 483 cm^{-1}, the rest of the vibrations contribute negligible amount to the PED. Most of the theoretically calculated in-plane and out-of-plane C-F assignments are consistent with the earlier reported values [72-74].

The O-H stretching vibrations occur starting from medium to strong intensity in the infrared spectrum and weak in the case of Raman spectra. The band is generally observed in the region around 3200-3650 cm^{-1} [68, 75-77]. Experimental data of the concerned molecule (4F4OHBP) reveals that the characteristic peak is observed at 3224 cm^{-1} in FT-IR spectrum. The theoretical vibrational assignments confirm that the O-H stretching vibration is observed at wavenumber 3681 cm^{-1}. It is also clear from PED that the hydroxyl stretching vibration is a completely pure mode as it contributes 100% to the PED. The in-plane O-H deformation vibration usually appears as a strong band in the region 1260-1440 cm^{-1} of the spectrum [70, 77], which gets shifted to higher wave number in the presence of hydrogen bonding. The theoretical calculation predicts that in-plane bending of the phenolic hydroxyl group (phII) is observed at 1145 and 1315 cm^{-1}.

Accepted Manuscript

The experimental data shows that FT-Raman spectrum is assigned at 1283 cm^{-1} and FT-IR spectra are observed at 1360, 1444, 1513 cm^{-1} for hydroxyl in-plane bending vibration of 4F4OHBP molecule. In various ortho-substituted phenol studies, the O-H out-of-plane bending vibrations are found in the frequency region 300–860 cm^{-1} [78]. In our case, the different hydroxyl vibrations such as stretching, in-plane bending and out-of-plane bending vibrations fall well within the expected range.

The C-C aromatic stretching vibrations give rise to characteristic bands in both the observed IR and Raman spectra, covering the spectral range from 650 to 1650 cm^{-1} [19, 70]. In this study, the bands identified at 193, 239, 355, 1077 cm^{-1} have been assigned as C-C stretching modes and the wavenumbers corresponding to C=C stretching vibrations are found within the range 193-1578 cm^{-1}. Among these modes, some of the vibrations are found below the usual region and this is arising due to the substitution of heavy substituent in the molecule. With heavy substituent, it has been observed that the vibration shifts towards the lower wavenumber site [19]. The major PED contribution is obtained at wavenumber of 1285 cm^{-1} (84%). The CCC in-plane bending modes are found at 148, 193, 239, 355, 537, 566, 617, 623, 641, 810, 988, 991, 1241 and 1573 cm^{-1} and the out-of-plane vibrations are noticed at wavenumbers 69, 266, 302, 483, 708 and 752 cm^{-1}. The most of CCC in-plane and out-of-plane assignments are matching well with the values available in the literature and also with the experimental findings [75-76]. This indicates that the substitutions made on both the phenyl rings (phI and phII) do not produce much influence to the vibrations of these modes. The results also confirm that CCC in-plane and out-of-plane vibrations are mixed modes as they consist of some other

Accepted Manuscript

vibrations such as C-H out-of-plane, O-H out-of-plane, C=O and C=C stretching vibrations.

Infrared Intensity And Raman Activities Analysis

In order to identify the proper functional groups of organic and inorganic compounds and also to study the reaction mechanism of new compounds, Infrared (IR) and Raman spectroscopic analysis are used as an effective tool [79]. It has been noticed that all the fundamental vibrations are active in IR absorption and Raman scattering. The IR intensity and Raman intensity computed using different functionals are presented in supporting information (Table S2). The average value of IR intensity calculated using HF method is higher than the DFT methods. But in case of DFT method the trend of average IR intensities calculated using three different functionals is found to be B3PW91 > CAM-B3LYP > B3LYP, whereas in case of Raman activities the trend is just reversed. This means that the average value of Raman activities computed using DFT method is higher than the HF method. It is found that B3LYP functional gives this highest average value of Raman activities as compare to other functionals used in this study. The recent literature survey reveals that Raman intensities are mostly used nowadays in comparison to Raman scattering activities. The comparative representation of experimental and simulated IR and Raman spectra are provided in Fig. 5.

Accepted Manuscript

CONCLUSIONS

In summary, DFT calculation using different functionals have been performed to investigate the structural, electronic, vibrational spectra and nonlinear optical property of

4-fluoro-4-hydroxybenzophenone molecule. The structural parameters computed using B3LYP and B3PW91 functionals are in close agreement with the available experimental data. As compare to gas phase, the dihedral angle between two benzene rings of 4F4OHBP molecule slightly increases in case of solvent phase. The UV-visible spectra analysis shows that the highest absorption peak of 4-fluoro-4-hydroxybenzophenone molecule is shifted towards the higher wavelength or lower energy side as we move from gas phase to solvent phase, which confirms the occurrence of red shift in the absorption spectra. The NLO properties of the molecule suggest that it is a good candidate for NLO applications and may help to design and synthesize new material with unique optical property as well. Finally, most of the vibrational assignments agree well with the experimental as well as earlier reported results.

ACKNOWLEDGEMENTS

Dr. U. Sarkar thanks, International Centre for Theoretical Physics, Trieste, Italy for hosting him as a regular associate. J. Deb thanks, Department of Science and Technology, New Delhi for providing him DST-INSPIRE Fellowship.

REFERENCES

[1] Linnemann, E. Uber Benzophenon und einige derivative desslben. *Annalen Der Chemie Und Pharmcie* **1865,** 133, 1-32.

[2] Sąsiadek, W.; Mączka, M.; Kucharska, E.; Hanuza, J.; Kaminskii, A. A.; Klapper, H. Polarized IR and Raman study and DFT chemical quantum calculations of the vibrational

Accepted Manuscript

levels for benzophenone single crystal. *Journal of Raman Spectroscopy* **2005**, 36, 912 – 923.

[3] Kaminskii, A. A.; Klapper, H; Hulliger, J.; Eichler, H. J.; Hanuza, J.; Ueda, K.; Takaichi, K.; Wickleder, C.; Gad, G. A. M.; Maczka, M. High-order many-phonon stimulated Raman scattering in orthorhombic benzophenone (C13H10O) and monoclinic alpha-4-methylbenzophenone (alpha-C14H12O) crystals. *Laser Physics* **2002**, 12, 1041-1053.

[4] Corrêa, B. A. M.; Gonçalves, A. S.; de Souza, A. M. T.; Freitas, C. A.; Cabral, L. M.; Albuquerque, M. G.; Castro, H. C; dos Santos, E. P.; Rodrigues, C. R. Molecular Modeling Studies of the Structural, Electronic, and UV Absorption Properties of Benzophenone Derivatives. *Journal of Physical Chemistry A* **2012**, 116, 10927−10933.

[5] Li, W. Q.; Zhang, Z. J.; Nan, X.; Liu, Y. Q.; Hu, G. F.; Yu, H. T.; Zhao, X. B.; Wu, D.; Yan, L. T. Design, synthesis and bioactivity evaluation of novel benzophenone hydrazone derivatives. *Pest Manag Sci* **2014**, 70, 667 – 673.

[6] Daoud-Mahammed, S.; Couvreur, P.; Bouchemal, K.; Chéron, M.; Lebas, G.; Amiel, C.; Gref, R. Cyclodextrin and Polysaccharide-Based Nanogels: Entrapment of Two Hydrophobic Molecules, Benzophenone and Tamoxifen. *Biomacromolecules* **2009**, 10, 547-554.

[7] Suzuki, T.; Kitamura, S.; Khota, R.; Sugihara, K.; Fujimoto, N.; Ohta, S. Estrogenic and antiandrogenic activities of 17 benzophenone derivatives used as UV stabilizers and sunscreens. *Toxicology and Applied Pharmacology* **2005**, 203, 9–17.

Accepted Manuscript

[8] Trakselis, M. A.; Alley, S. C.; Ishmaez, F. T. Identification and Mapping of Protein-Protein Interactions by a Combination of Cross-Linking, Cleavage, and Proteomics. *Bioconjugate Chemistry* **2005,** 16, 741-750.

[9] Dormán, G.; Prestwich, G. D. Benzophenone Photophores in Biochemistry. *Biochemistry* **1994**, 33, 5661-5673.

[10] Islam, N; Pandith, A. H. Analysis of vibrational spectra (FT-IR and VCD) and nonlinear optical properties of $[Ru(L)_3]^{2+}$complexes. *Journal of Coordination Chemistry* **2014**, 67, 3288-3310.

[11] Li, Y.; Zhang, Y.; Qi, D.; Sun, C.; Yan, L. Nonlinear optical properties and performance optimization of the pro-aromatic chromophores for NLO materials. *Journal of Materials Science: Materials in Electronics* **2014**, 25, 5255–5263.

[12] Gümüs, H. P.; Tamer, Ö.; Avci, D.; Tarcan, E.; Atalay, Y. Theoretical Investigations on Nonlinear Optical and Spectroscopic Properties of 6-(3,3,4,4,4-Pentafluoro-2-hydroxy-1-butenyl)-2,4-pyrimidinedione: An Efficient NLO Material[1]. *Russian Journal of Physical Chemistry A* **2014**, 88, 2348-2358.

[13] Islam, N.; Niaz, S.; Manzoor, T.; Pandith, A. H. Theoretical investigations into spectral and non-linear optical properties of brucine and strychnine using density functional theory. *Spectrochimica Acta Part A: Molecular and Bimolecular Spectroscopy* **2014**, 131, 461-470.

[14] Islam, N.; Pandith, A. H. Optoelectronic and nonlinear optical properties of triarylamine helicenes: a DFT study. *Journal of Molecular Modeling* **2014**, 20, 2535(1/17).

Accepted Manuscript

[15] Pandith, A. H.; Islam, N. Electron Transport and Nonlinear Optical Properties of Substituted Aryldimesityl Boranes: A DFT Study. *PLOS ONE* **2014**, DOI: 10.1371/journal.pone.0114125.

[16] Prasad, P. N.; Williams, D. J. Introduction to Nonlinear Optical Effects in Molecules and Polymers; Press: Wiley, NewYork, **1991**; 320 pp.

[17] Sethuraman, K.; Babu, R. R.; Vijayan, N.; Gopalakrishnan, R.; Ramasamy, P. Synthesis, Growth of Organic nonlinear optical crystal: Semicarbazone of 2-Amino-5-Chloro-Benzophenone (S2A5CB) and its Characterization. *Journal of Crystal Growth* **2006**, 290**,** 539-543.

[18] Ranson, P.; Peretti, P.; Rousset, Y.; Koningstein, J. A. Low-frequency raman spectrum of benzophenone at 300 and 30°K. *Chemical Physics Letters* **1972**, 16, 396-398.

[19] Chaitanya, K.; Santhamma, C.; Heron, B. M.; Gabbutt, C. D.; Instone, A. C. Vibrational assignment of the spectral data and thermodynamic properties of 2-chloro-4-fluorobenzophenone using DFT quantum chemical calculations. *Vibrational Spectroscopy* **2011**, 57, 35–41.

[20] Giorgianni, S.; Passerini, A.; Gambi, A.; Ghersetti, S.; Spunta, G. Infrared Spectra of Benzophenone and Its p-Halogen Derivatives. *Spectroscopy Letters* **1980**, 13, 445-455.

[21] Blažević, J.; Colombo, L. The vibrational spectrum of the benzophenone molecule. *Journal of Raman Spectroscopy* **1981**, 11, 143-149.

[22] Mathur, M. S.; Nelson, J. B.; Tabisz, G. C. Far-Infrared Spectrum of Benzophenone. *Spectroscopy Letters* **1981**, 14, 339-346.

Accepted Manuscript

[23] Kolev, T. M.; Stamboliyska, B. A. Vibrational spectra and structure of benzophenone and its 18_O and d_{10} labelled derivatives: an ab initio and experimental study. *Spectrochimica Acta Part A: Molecular and Bimolecular Spectroscopy* **1999**, 56, 119-126.

[24] Sett, P.; Misra, T.; Chattopadhyay, S.; De, A. K.; Mallick, P.K. DFT calculation and Raman excitation profile studies of benzophenone molecule. *Vibrational Spectroscopy* **2007**, 44, 331-342.

[25] Volovšek, V.; Baranović, G.; Colombo, L. Normal coordinate analysis of the halogenated disubstituted benzophenones. *Journal of Molecular Structure* **1992**, 266, 217-222.

[26] Vachev, V. D.; Frederick, J. H. The (n, $\pi*$) absorption spectrum of benzophenone. A new model for the excited state dynamics. *Chemical Physics Letters* **1996**, 249, 476-484.

[27] Krishnakumar, V.; Muthunatesan, S.; Keresztury, G.; Sundius, T. Scaled quantum chemical calculations and FTIR, FT-Raman spectral analysis of 3,4-diamino benzophenone. *Spectrochimica Acta Part A: Molecular and Biomolecular Spectroscopy* **2005**, 62, 1081-1088.

[28] Jr., M. V.; Tanaka, J. Aromatic Carbonyl Spectra. I. The Polarized Absorption Spectrum of Single- Crystal 4,4′- Dichlorobenzophenone. *The Journal of Chemical Physics* **1968**, 49, 5222-5234.

[29] Barone, V.; Baiardi, A.; Biczysko, M.; Bloino, J.; Cappelli, C.; Lipparini, F. Implementation and validation of a multi-purpose virtual spectrometer for large systems in complex environments. *Physical Chemistry Chemical Physics* **2012**, 14, 12404–12422.

Accepted Manuscript

[30] Barone, V.; Biczysko, M.; Bloino, J. Fully anharmonic IR and Raman spectra of medium-size molecular systems: accuracy and interpretation. *Physical Chemistry Chemical Physics* **2014**, 16, 1759-1787.

[31] SDBS Web: http://sdbs.db.aist.go.jp (National Institute of Advanced Industrial Science and Technology).

[32] Krishnan, R.; Binkley, J. S.; Seeger, R.; Pople, J. A. Self-consistent molecular orbital methods. XX. A basis set for correlated wave functions. *The Journal of Chemical Physics* **1980**, 72, 650-654.

[33] Dennington, R.; Keith, T.; Millam, J. *GAUSSVIEW, Version 5*; Semichem Inc.: Shawnee Mission, KS, **2009**.

[34] Martin, J. M. L; Van Alsenoy, C. *GAR2PED, A Program to Obtain a Potential Energy Distribution from a Gaussian Archive Record;* University of Antwerp, Belgium, **2007**.

[35] Parr, R. G.; Yang, W. Density-Functional Theory of the Electronic Structure of Molecules. *Annual Review of Physical Chemistry* **1995**, 46, 701-728.

[36] Parr, R. G.; Pearson, R. G. Absolute hardness: companion parameter to absolute electronegativity. *Journal of the American Chemical Society* **1983**, 105, 7512–7516.

[37] Chattaraj, P. K.; Sarkar, U.; Roy, D. R. Electrophilicity Index. *Chemical Reviews* **2006**, 106, 2065−2091.

[38] Parr, R. G.; Szentpály L. V.; Liu, S. *Journal of the American Chemical Society* **1999**, 121, 1922-1924.

[39] Keresztury, G.; Holly, S.; Varga, J.; Besenyei, G.; Wang, A. Y.; Durig, J. R. Vibrational spectra of monothiocarbamates-II. IR and Raman spectra, vibrational

Accepted Manuscript

assignment, conformational analysis and *ab initio* calculations of *S*-methyl-N, N-dimethylthiocarbamate. *Spectrochimica Acta Part A: Molecular Spectroscopy* **1993**, 49, 2007-2026.

[40] Prodic, B. K.; Pahor, N. B.; Horvatic, D. Structure of 4,4'-dimethylbenzophenone. Acta Crystallographic 1990, C46, 430-432.

[41] Sundaraganesan, N.; Kalaichelvan, S.; Meganathan, C.; Joshua, B. D.; Cornard, J. FT-IR, FT-Raman spectra and ab initio HF and DFT calculations of 4-N, N/-dimethylamino pyridine. *Spectrochimica Acta Part A: Molecular and Biomolecular Spectroscopy* **2008**, 71, 898–906.

[42] Mahadevana, D.; Periandy, S.; Ramalingam, S. Comparative vibrational analysis of 1,2-Dinitro benzene and 1-Fluoro-3-nitro benzene: A combined experimental (FT-IR and FT-Raman) and theoretical study (DFT/B3LYP/B3PW91). *Spectrochimica Acta Part A: Molecular and Biomolecular Spectroscopy* **2011**, 84, 86–98.

[43] Cox, P. J.; Kechagias, D.; Kelly, O. Conformations of substituted benzophenones. *Acta Crystallographica Section B* **2008**, 64, 206-216.

[44] Ghara, M.; Pan, S.; Deb, J.; Kumar, A.; Sarkar, U.; Chattaraj, P. K. A computational study on structure, stability and bonding in Noble Gas bound metal Nitrates, Sulfates and Carbonates (Metal = Cu, Ag, Au). *Journal of Chemical Sciences* **2016**, 10, 1537-1548.

[45] Parr, R. G., Chattaraj, P. K. Principle of maximum hardness**.** *Journal of the American Chemical Society* **1991**, 113, 1854-1855.

[46] Ravikumar, C.; Joe, I. H.; Jayakumar, V. S. Charge transfer interactions and nonlinear optical properties of push–pull chromophore benzaldehyde phenylhydrazone: A vibrational approach. *Chemical Physics Letters* **2008**, 460, 552-558.

Accepted Manuscript

[47] Migahed, M. A.; Zaki, E. G.; Shaban, M. M. Corrosion control in oil wells tubing steel during matrix acidizing operations. *The Royal Society of Chemistry Advances* **2016**, 6, 71384-71396.

[48] Elango, M.; Parthasarathi, R.; Subramanian, V.; Sarkar, U.; Chattaraj, P. K. Formaldehyde decomposition through profiles of global reactivity indices. *Journal of Molecular Structure: THEOCHEM* **2005**, 723, 43-52.

[49] Khatua, M.; Sarkar, U.; Chattaraj, P. K. Reactivity dynamics of confined atoms in the presence of an external magnetic field. *The European Physical Journal D* **2014**, 68, 22(1/9).

[50] Chattaraj, P. K.; Sarkar, U. Chemical reactivity dynamics in ground and excited electronic states. *Theoretical and Computational Chemistry* **2007**, 19, 269-286.

[51] Chattaraj, P. K.; Sarkar, U. Ground- and Excited-States Reactivity Dynamics of Hydrogen and Helium Atoms. *International Journal of Quantum* Chemistry **2003**, 91, 633-650.

[52] Sarkar, U.; Khatua, M.; Chattaraj, P. K. A tug-of-war between electronic excitation and confinement in a dynamical context. *Physical Chemistry Chemical Physics* **2012**, 14, 1716-1727.

[53] Sarkar, U.; Padmanabhan, J.; Parthasarathi, R.; Subramanian, V. Toxicity analysis of polychlorinated dibenzofurans through global and local electrophilicities. *Journal of Molecular Structure: THEOCHEM* **2006**, 758, 119-125.

[54] Sarkar, U.; Roy, D. R.; Chattaraj, P. K.; Parthasarathi, R.; Padmanabhan, J. A conceptual DFT approach towards analysing toxicity. *Journal of Chemical Sciences* **2005**, 117, 599-612.

Accepted Manuscript

[55] Chattaraj, P. K.; Sarkar, U.; Roy, D. R. Electronic Structure Principles and Aromaticity. *Journal of Chemical Education* **2007**, 84, 354-357.

[56] Chattaraj, P. K.; Sarkar, U.; Parthasarathi, R.; Subramanian, V. DFT study of some aliphatic amines using generalized philicity concept. *International Journal of Quantum Chemistry* **2005**, 101, 690-702.

[57] Roy, D. R.; Parthasarathi, R.; Padmanabhan, J.; Sarkar, U; Subramanium, V.; Chattaraj, P. K. Careful Scrutiny of the Philicity Concept. *The Journal of Physical Chemistry A* **2006**, 110, 1084-1093.

[58] Singh, N. B.; Sarkar, U. Structure, vibrational, and optical properties of platinum cluster: a density functional theory approach. *Journal of Molecular Modeling* **2014,** 20, 2537(1/11).

[59] Koopmans, T. A. Über die Zuordnung von Wellenfunktionen und Eigenwerten zu den Einzelnen Elektronen Eines Atoms. *Physica* **1934**, 1, 104-113.

[60] Pandith, A. H. Islam, N. Comparative Assessment of QSTR Models Based on Density Functional, Hartree–Fock, AM1, and PM3 Methods for Acute Toxicity of Aliphatic Compounds Toward Vibrio fischeri. *International Journal of Quantum* Chemistry **2013**, 113, 830–839.

[61] Chamorro, E.; Chattaraj, P. K.; Fuentealba, P. Variation of the Electrophilicity Index along the Reaction Path," *The Journal of Physical Chemistry A* **2003**, 107, 7068–7072.

[62] Geskin, V. M.; Lambert, C.; Brédas, J. L. Origin of High Second- and Third-Order Nonlinear Optical Response in Ammonio/Borato Diphenylpolyene Zwitterions: the Remarkable Role of Polarized Aromatic Groups. *Journal of the American Chemical Society* **2003**, 125, 15651–15658.

Accepted Manuscript

[63] Sajan, D.; Joe, I. H.; Jayakumar, V. S.; Zaleski, J. Structural and electronic contributions to hyperpolarizability in methyl p-hydroxy benzoate. *Journal of Molecular Structure* **2006**, 785, 43–53.

[64] Kanis, D. R.; Ratner, M. A.; Marks, T. J. Design and Construction of Molecular Assemblies with Large Second-Order Optical Nonlinearities. Quantum Chemical Aspects. *Chemical Reviews* **1994**, 94, 195–242.

[65] Bredas, J. L.; Adant, C.; Tackx, P.; Persoons, A. Third-Order Nonlinear Optical Response in Organic Materials: Theoretical and Experimental Aspects. *Chemical Reviews* **1994**, 94, 243-278.

[66] Karabacaka, M.; Çınar, M.; Çoruh, A.; Kurt, M. Theoretical investigation on the molecular structure, Infrared, Raman and NMR spectra of *para*-halogen benzenesulfonamides, 4-X-$C_6H_4SO_2NH_2$ (X = Cl, Br or F). *Journal of Molecular Structure* **2009**, 919, 26–33.

[67] Alaşalvar, C.; Demircan, A.; Koşar, B.; Pekacar, A.İ.; Büyükgüngör, O. Crystal structure, spectroscopic investigations and quantum chemical calculation studies of (3a*R*,6*S*,7a*R*)-7a-bromo-6-methyl-2-[(4-methylphenyl)sulfonyl]-1,2,3,6,7,7a-hexahydro-3a,6-epoxyisoindole: A combined experimental and theoretical studies. *Journal of Molecular Structure* **2016**, 1123, 213-224.

[68] Qian, W.; Krimm, S. Dipole Derivative Distribution: A Useful Adjunct to the Potential Energy Distribution. *Journal of Physical Chemistry* **1993**, 97, 11578-11579.

[69] George, W. O.; Mcintyre, P. S. Infrared spectroscopy: Analytical chemistry by open learning; Press: John Wiley & Sons, London, **1987**.

Accepted Manuscript

[70] Varsányi, G. Assignments for Vibrational Spectra of Seven Hundred Benzene Derivatives, volumes 1 and 2; Press: Adam Hilger, London, **1974**.

[71] Sajan, D.; Joe, I.H.; Jayakumar, V.S. NIR-FT Raman, FT-IR and surface-enhanced Raman scattering spectra of organic nonlinear optic material: *p*-hydroxy acetophenone. *Journal of Raman Spectroscopy* **2006**, 37, 508-519.

[72] Eatch, V. J.; Steel, D. The vibrational force field of halogenated aromatic molecules: In-plane vibrations of benzene and fluorobenzenes. *Journal of Molecular Spectroscopy* **1973**, 48, 446–449.

[73] Ramalingam, S.; Periandy, S.; Elanchezhian, B.; Mohan, S. FT-IR and FT-Raman spectra and vibrational investigation of 4-chloro-2-fluoro toluene using ab initio HF and DFT (B3LYP/B3PW91) calculations. *Spectrochimica Acta Part A: Molecular and Biomolecular Spectroscopy* 2011, 78, 429–436.

[74] Sundaraganesana, N.; Meganathan, C.; Joshua, B. D.; Mani, P.; Jayaprakash, A. Molecular structure and vibrational spectra of 3-chloro-4-fluoro benzonitrile by ab initio HF and density functional method. *Spectrochimica Acta Part A: Molecular and Biomolecular Spectroscopy* **2008**, 71, 1134–1139.

[75] Karabacak, M.; Cinar, Z.; Kurt, M.; Sudha, S.; Sundaraganesan, N. FT-IR, FT-Raman, NMR and UV–vis spectra, vibrational assignments and DFT calculations of 4-butyl benzoic acid. *Spectrochimica Acta Part A: Molecular and Biomolecular Spectroscopy* **2012**, 85, 179-189.

[76] Arjunan, V.; Kalaivani, M.; Ravindran, P.; Mohan, S. Structural, vibrational and quantum chemical investigations on 5-chloro-2-hydroxybenzamide and 5-chloro-2-

Accepted Manuscript

hydroxybenzoic acid. *Spectrochimica Acta Part A: Molecular and Biomolecular Spectroscopy* **2011**, 79, 1886–1895.

[77] Arjunan, V.; Mohan, S.; Ravindran, P.; Mythili, C. V. Vibrational spectroscopic investigations, ab initio and DFT studies on 7-bromo-5-chloro-8-hydroxyquinoline. *Spectrochimica Acta Part A: Molecular and Biomolecular Spectroscopy* **2009**, 72, 783–788.

[78] Nyquist, R. A. The O-H out-of-plane deformation in intramolecularly hydrogen bonded phenols. *Spectrochimica Acta Part A: Molecular and Biomolecular Spectroscopy* **1963**, 19, 1655-1684.

[79] Andrianov, V.M.; Korolevich, M.V. CALCULATION AND COMPARATIVE ANALYSIS OF THE IR SPECTRA OF HOMOBRASSINOLIDE AND (22S, 23S)-HOMOBRASSINOLIDE. *Journal of Applied Spectroscopy* **2015**, 82, 521-531.

Accepted Manuscript

Table 1. Structural parameters (bond length, bond angles and dihedral angles) of 4-fluoro-4-hydroxybenzophenone determined with HF, B3LYP, B3PW91 and CAM-B3LYP using 6-311++G(d,p) basis set.

Bond length (Å)	HF	B3LYP	B3PW91	CAM-B3LYP	Experimental value
C1–C2	1.39	1.40	1.40	1.39	1.39
C2–C3	1.38	1.39	1.39	1.38	1.38
C3-C4	1.38	1.39	1.39	1.38	1.38
C4–C5	1.37	1.38	1.38	1.38	1.39
C5–C6	1.38	1.39	1.39	1.39	1.39
C6-C1	1.39	1.40	1.40	1.39	-
C2-H7	1.07	1.08	1.08	1.08	-
C3-H8	1.07	1.08	1.08	1.08	-
C4-F9	1.32	1.35	1.34	1.35	-
C5-H10	1.07	1.08	1.08	1.08	-
C6-H11	1.07	1.08	1.08	1.08	-
C1-C12	1.50	1.50	1.50	1.50	-
C12-O13	1.19	1.22	1.22	1.21	1.23
C12-C14	1.49	1.49	1.49	1.49	1.50
C14-C15	1.39	1.40	1.40	1.39	1.39
C15-C16	1.38	1.39	1.38	1.38	1.40
C16-C17	1.39	1.40	1.40	1.39	1.35
C17-C18	1.39	1.40	1.39	1.39	1.37
C18-C19	1.38	1.39	1.39	1.38	1.41

Accepted Manuscript

C19-C24	1.07	1.08	1.08	1.08	-
C15-H20	1.07	1.08	1.08	1.08	-
C16-H21`	1.08	1.09	1.09	1.08	-
C17-O25	1.34	1.36	1.36	1.36	-
O25-H22	0.94	0.96	0.96	0.96	-
C18-H23	1.07	1.08	1.08	1.08	-
C19-H24	1.07	1.08	1.08	1.08	-
Bond angles (^{0})					
C1-C2-C3	120.89	120.91	120.90	120.82	121.37
C2-C3-C4	118.42	118.38	118.41	118.31	118.57
C3-C4-C5	122.39	122.49	122.41	122.58	122.22
C4-C5-C6	118.46	118.41	118.44	118.38	118.03
C3-C4-F9	118.77	118.74	118.78	118.70	118.52
C4-C5-H10	119.89	119.85	119.81	119.77	120.04
C5-C6-H11	118.91	119.13	119.25	119.22	119.27
C2-C1-C12	118.04	118.04	118.03	117.92	122.78
C1-C12-O13	119.47	119.51	119.66	119.53	120.14
C1-C12-C14	120.33	119.51	119.89	120.18	118.94
O13-C12-C14	120.20	120.31	120.45	120.29	120.89
C12-C14-C15	118.17	118.14	118.11	118.03	117.55
C14-C15-C16	121.06	120.99	120.95	120.91	120.40
C15-C16-C17	119.68	119.77	119.80	119.69	119.99
C16-C17-C18	120.11	120.08	120.02	120.18	120.03

Accepted Manuscript

C17-C18-C19	119.59	119.64	119.66	119.61	120.07
C14-C15-C20	119.01	118.61	118.54	118.60	-
C16-C15-C20	119.93	120.39	120.51	120.49	-
C15-C16-H21	120.15	120.22	120.20	120.27	-
C17-C16-H21	120.17	120.00	119.99	120.03	-
C16-C17-O25	122.36	122.55	122.52	122.44	-
C18-C17-O25	117.53	117.37	117.45	117.38	-
C17-O25-H22	111.35	110.04	109.75	110.32	-
C17-C18-H23	119.18	119.06	119.03	118.98	-
C19-C18-H23	121.22	121.30	121.31	121.40	-
C18-C19-H24	118.66	118.91	119.02	118.99	-
C14-C19-H24	120.18	119.98	119.90	120.02	-
Dihedral angles (^{0})					
C2-C1-C12-O13	30.81	29.39	29.34	29.29	
C6-C1-C12-C14	30.81	33.52	33.50	33.22	
O13-C12-C14-C15	26.51	24.86	24.83	25.12	
C1-C12-C14-C19	30.44	28.99	29.03	29.10	
H22-O25-C17-C16	-0.87	-0.70	-0.65	-0.67	
C6-C1-C14-C19	54.03	51.91	51.95	51.81	
H8-C3-C4-F9	0.11	0.03	0.04	0.09	

Accepted Manuscript

Table 2. Dihedral angles of 4-fluoro-4-hydroxybenzophenone for different solvent phases determined with B3LYP functional using 6-311++G(d,p) basis set.

Dihedral angle (^{0})	Gas	Chloroform	Ethanol	DMSO
C2-C1-C12-O13	29.39	31.06	31.77	31.87
C6-C1-C12-C14	33.52	34.92	35.55	35.64
O13-C12-C14-C15	24.86	25.30	25.23	25.21
C1-C12-C14-C19	28.99	29.14	28.92	28.88
H22-O25-C17-C16	-0.70	-0.66	-0.50	-0.47
C6-C1-C14-C19	51.91	53.37	53.76	53.81
H8-C3-C4-F9	0.03	-0.14	-0.23	-0.25

Accepted Manuscript

Table 3. The energy gap (E_{LUMO}- E_{HOMO}), chemical reactivity parameters (ionization potential, electron affinity, chemical hardness, chemical potential and electrophilicity index) computed using various functional of the 4-fluoro-4-hydroxybenzophenone molecule.

Reactivity parameters	**HF**	**B3LYP**	**B3PW91**	**CAM-B3LYP**
Energy gap (E_g) (eV)	9.945	4.717	4.742	7.399
Ionization potential (I) (eV)	9.058	6.779	6.802	8.192
Electron affinity (A) (eV)	-0.887	2.062	2.060	0.792
Chemical hardness(η) (eV)	9.945	4.717	4.742	7.400
Chemical potential (μ) (eV)	-4.086	-4.421	- 4.431	-4.492
Electrophilicity index (ω) (eV)	0.839	2.071	2.070	1.364

Accepted Manuscript

Table 4. Nonlinear optical properties (dipole moment, polarizability and first hyperpolarizability) calculated using different functionals for 4-fluoro-4-hydroxybenzophenone molecule.

Parameters	HF	B3LYP	B3PW91	CAM-B3LYP
α_{xx} (a.u.)	152.924	172.123	168.301	222.124
α_{xy} (a.u.)	8.384	7.807	8.096	-3.289
α_{yy} (a.u.)	108.243	113.526	111.079	149.718
α_{xz} (a.u.)	32.171	44.106	42.274	10.862
α_{yz} (a.u.)	-22.630	-30.198	-29.328	-0.507
α_{zz} (a.u.)	174.414	201.441	197.355	96.394
α (e.s.u.)	1.254×10^{-30}	1.403×10^{-30}	1.373×10^{-30}	1.348×10^{-30}
$\Delta\alpha$ (a.u.)	363.921	410.948	401.913	387.927
μ_x (Debye)	-0.056	-0.076	-0.057	0.972
μ_y (Debye)	-0.263	-0.306	-0.290	-0.531
μ_z (Debye)	-1.077	-1.127	-1.133	0.223
μ (Debye)	1.110	1.171	1.171	1.130
β_{xxx} (a.u.)	225.138	435.463	404.252	-282.588
β_{xxy} (a.u.)	1.941	22.410	18.492	602.648
β_{xyy} (a.u.)	-59.916	-79.369	-73.427	-44.050
β_{yyy} (a.u.)	5.741	43.476	38.653	-6.199
β_{xxz} (a.u.)	186.100	287.940	275.504	24.701
β_{xyz} (a.u.)	93.111	153.529	140.122	15.411
β_{yyz} (a.u.)	-74.322	-151.428	-139.743	-1.284

Accepted Manuscript

β_{xzz} (a.u.)	-32.823	-80.586	-67.047	4.882
β_{yzz} (a.u.)	211.445	400.210	372.310	-8.475
β_{zzz} (a.u.)	-383.985	-774.002	-725.625	2.921
β (e.s.u)	3.228×10^{-30}	7.226×10^{-30}	6.703×10^{-30}	5.795×10^{-30}

Accepted Manuscript

Table 5. The UV-visible excitation energy, maximum absorption wavelength, oscillator strength and major electronic transitions of 4-fluoro-4-hydroxybenzophenone molecule.

	Absorption wavelength λ (nm)	Excitation energy E (eV)	Oscillator strength f	Major electronic transitions
Gas	337.0	3.68	0.003	H-1→LUMO (45%), H-2→LUMO (24%)
	286.6	4.33	0.287	HOMO→LUMO (60%), H-1→LUMO (28%)
	264.4	4.69	0.004	H-3→LUMO (57%), HOMO→L+1 (19%)
Chloroform	327.3	3.79	0.012	H-1→LUMO (36%) H-3→LUMO (24%)
	298.9	4.15	0.387	HOMO→LUMO (68%), H-1→LUMO (20%)
	270.0	4.59	0.007	H-2→LUMO (51%), H-3→LUMO (27%)
Ethanol	323.4	3.83	0.019	H-1→LUMO (30%), H-1→LUMO (25%)
	301.2	4.11	0.368	H-1→LUMO (19%), HOMO→LUMO (67%)
	272.3	4.56	0.007	H-3→LUMO (13%), H-2→LUMO (67%)

Accepted Manuscript

DMSO	323.5	3.83	0.024	H-1→LUMO (29%), H-3→LUMO (24%)
	302.4	4.10	0.388	HOMO→LUMO (66%), H-1→LUMO (20%)
	272.6	4.55	0.008	H-2→LUMO (69%), H-2→LUMO (69%)

Accepted Manuscript

Table 6. Vibrational assignments of observed, calculated (scaled) frequencies with different functional and the percentage of potential energy distribution of 4-fluoro-4-hydroxybenzophenone molecule.

Obs. nos	Experimental		HF/6-311++G(d,p)	B3LYP/6-311++G(d,p)	B3PW91/6-311++G(d,p)	CAM-B3LYP/6-311G++(d,p)	Assignments (PED ≥ 10%)
	IR ν (cm^{-1})	Raman ν (cm^{-1})					
1	-	-	35	37	37	38	τ[(CCCC) (CCCO)] (89)
2	-	-	52	52	52	54	τ(CCCC) (30), δ(CCC) (53)
3	-	59	69	69	69	72	τ[(CCCC) (CCCO)] (37), τ(CCCC) (phI) (14), τ(CCCC) (phII) (14), ɣ(CCCC) (16),
4	-	84	104	99	99	104	τ[(CCCC) (CCCO)] (45), τ(CCCC) (phII) (12)
5	-	119	151	148	147	154	τ(CCCC) (phI) (20), τ(CCCC) (phII) (18), δ(CCC) (23), ɣ(FCCC) (phI) (10)
6	-	161	196	193	190	199	δ(CCC) (56), ɣ(FCCC) (phI) (10)
7	-	-	239	239	238	247	ν(C-C) (26) s, δ(CCC) (phI) (13), δ(CCC) (phII) (12), δ(CCC) (19)

Accepted Manuscript

8	-		274	266	263	276	ɣ(CCCC) (28), τ(CCCC) (phI) (10), τ(CCCC) (phII) (28)
9	-	270	295	302	300	314	ɣ(CCCC) (32), τ(CCCC) (phI) (17), τ(CCCC) (phII) (15), δ(CFC) (phI) (12)
10	-	318	313	335	343	340	τ(HOCC) (phII) (91), δ(CFC) (phI) (10)
11	-	-	359	355	353	367	ν(C-C) (17) as, δ(COC) (21), δ(CCC) (phI) (15), δ(CCC) (phII) (18), δ(CFC) (phI) (10)
12	-	-	401	391	389	404	δ(CFC) (phI) (30), δ(COC) (phII) (26)
13	-	-	411	402	399	415	δ(CFC) (phI) (18), δ(COC) (phII) (24), τ(CCCC) (phI) (13), τ(CCCC) (phII) (15)
14	-	-	416	406	403	421	τ(CCCC) (phI) (27), τ(CCCC) (phII) (44)
15	-	-	425	416	413	431	τ(CCCC) (phI) (48), τ(CCCC) (phII) (31)
16	-	-	493	483	482	501	ɣ(FCCC) (phI) (31), τ(CCCC) (phI) (36), ɣ(CCCC) (10)
17	-	-	504	488	486	506	ɣ(OCCC) (phII) (31), τ(CCCC)

Accepted Manuscript

							(phII) (35), τ(CCCC) (11),
18	491	-	550	537	534	555	δ[(CCC) (COC)] (18), ɣ(FCCC) (phI) (10), ɣ(OCCC) (phII) (10)
19	511	-	573	566	563	585	δ(COC) (23), δ(CCC) (phII) (17), δ(CCC) (phI) (14)
20	584	568	623	617	611	636	δ(CCC) (phI) (67)
21	-	-	627	623	617	642	δ(CCC) (phII) (59)
22	-	-	646	641	640	663	ν(C-C) (16) s, δ(CCC) (phII) (21)
23	-	-	683	662	660	687	τ(CCCC) (phI) (31), τ(CCCC) (phII) (28)
24	666	666	725	708	705	736	τ(CCCC) (phI) (33), τ(CCCC) (phII) (32), ɣ(CCCC) (12)
25	685	-	780	752	750	783	τ(CCCC) (phII) (19), ɣ(OCCC) (19), ɣ(CCCC) (12)
26	-	-	801	791	788	820	ν(C-F) (phI) (12), ɣ(HCCC) (11), δ(CCC) (phI) (17)
27	-	-	818	793	791	826	ɣ(HCCC) (phII) (75)
28	-	-	828	801	797	834	ɣ(HCCC) (phI) (95)
29	770	-	840	810	810	842	δ(CCC) (phII) (11), ν(C-O) (phII) (11), ν(C-C) (phII) (16) s
30	811		855	822	819	856	ɣ(HCCC) (phII) (51)

Accepted Manuscript

31	819	836	871	837	833	872	τ(CCCC) (phI) (10), ɣ(CHCC) (phI) (52)
32	-	-	912	905	904	940	δ(COC) (20), ν(C-C) (phI) (10), ν(C-C) (phII) (10) as
33	840	-	977	933	926	974	τ(CCCC) (phII) (12), ɣ(HCCC) (phI) (54), ɣ(HCCC) (phII) (18)
34	848	-	980	934	928	976	τ(CCCC) (phII) (12), ɣ(HCCC) (phI) (13), ɣ(HCCC) (phII) (52),
35	866	-	996	947	941	989	ɣ(HCCC) (phI) (34), ɣ(HCCC) (phII) (53),
36	930	-	999	952	947	994	ɣ(HCCC) (phI) (56), ɣ(HCCC) (phII) (30),
37	-	-	1001	988	982	1020	ν(C-C) (phII) (36) s, δ(CCC) (phII) (44)
38	-	-	1002	991	985	1022	ν(C-C) (phI) (36) s, δ(CCC) (phI) (44)
39	-	-	1061	1077	1070	1105	δ(CHC) (phI) (62), ν(C-C) (phI) (28) as
40	-	-	1078	1085	1078	1115	δ(CHC) (phII) (55), ν(C-C) (phII) (24) as
41	1118	-	1120	1121	1122	1160	ν(C-C) (29) as

Accepted Manuscript

42	-	-	1130	1130	1123	1162	δ(CHC) (phI) (65)
43	-	-	1147	1145	1141	1172	δ(CHO) (phII) (45), δ(CHC) (phII) (15), ν(C-C) (phII) (20) as
44	1148	1146	1161	1149	1143	1179	δ(CHC) (phII) (63)
45	1168	-	1164	1196	1204	1245	ν(C-C) (phI) (17) as, ν(C-F) (49), δ(CHC) (phI) (15), δ(CCC) (phI) (11)
46	1175		1224	1237	1245	1285	ν(C-C) (phII) (14), ν(C-C) (29) as, ν(C-O) (27)
47	1230	-	1237	1241	1248	1287	ν(C-C) (25) as, ν(C-O) (23), δ(CCC) (phII) (13)
48	1287		1259	1270	1257	1302	δ(CHC) (phI) (84)
49	1299	-	1272	1282	1277	1308	ν(C-C) (phII) (26) as, δ(CHC) (phII) (40)
50	1315	1227	1295	1285	1304	1317	ν(C-C) (phI) (84) as
51	1360	1283	1321	1315	1326	1341	ν(C-C) (phII) (60) as, δ(CHO) (phII) (15), δ(CHC) (phII) (22)
52	1408	-	1399	1379	1378	1428	ν(C-C) (phI) (47) as, δ(CHC) (phI) (37)
53	1444	-	1424	1403	1402	1452	ν(C-C) (phII) (40) as, δ(CHC) (phII) (29)
54	1505		1511	1472	1470	1527	ν(C-C) (phI) (30) as, δ(CHC) (phI)

Accepted Manuscript

							(45)
55	1562	-	1519	1479	1479	1536	ν(C-C) (phII) (30) as, δ(CHC) (phII) (42)
56	1513		1598	1558	1564	1628	ν(C-C) (phII) (73) as
57	1572	1561	1600	1561	1568	1632	ν(C-C) (phI) (69) as
58	1586	1583	1619	1573	1581	1645	ν(C-C) (phI) (54) as, δ(CCC) (phI) (10), δ(CHC) (phI) (10),
59	1604	1606	1623	1578	1586	1648	ν(C-C) (phII) (52) as
60	1637	1631	1737	1639	1653	1726	ν(C=O) (73)
61	-	-	3001	3032	3028	3116	ν(C-H) (phII) (96) as
62	3032	-	3029	3063	3056	3144	ν(C-H) (phI) (12) as , ν (C-H) (phII) (84) as,
63	-	-	3032	3066	3059	3148	ν(C-H) (phI) (79) as, ν (C-H) (phII) (10) as
64	-	-	3036	3070	3064	3151	ν(C-H) (phI) (93) as
65	-	-	3044	3074	3068	3155	ν(C-H) (phII) (93) s
66	3072	-	3046	3077	3072	3159	ν(C-H) (phII) (92) s
67	3203	-	3047	3080	3076	3163	ν(C-H) (phI) (91) as
68	3213	3078	3051	3082	3077	3164	ν(C-H) (phI) (96) s
69	3224	-	3785	3681	3692	3795	ν(O-H) (phII) (100)

ν- stretching; δ- in-plane bending; ϒ- out-of plane bending; τ- torsion; as- asymmetric; s- symmetric

Accepted Manuscript

Figure 1. Optimized geometry of 4-fluoro-4-hydroxybenzophenone molecule.

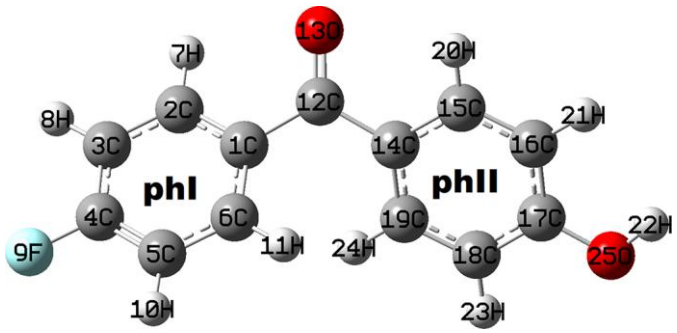

Accepted Manuscript

Figure 2. Molecular orbital plot of 4-fluoro-4-hydroxybenzophenone molecule.

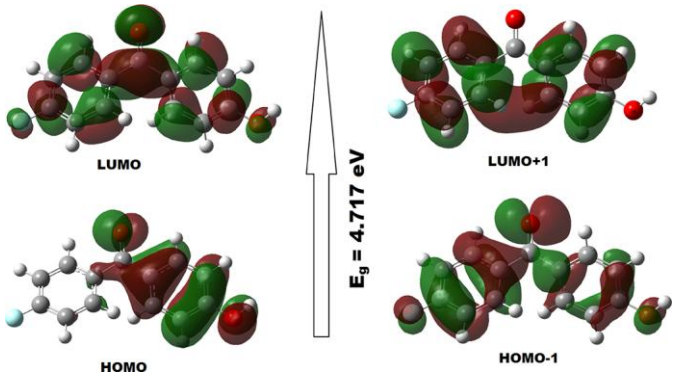

Accepted Manuscript

Figure 3. (a) Molecular electrostatic potential; (b) Total electron density; (c) Electrostatic potential plot of 4-fluoro-4-hydroxybenzophenone molecule.

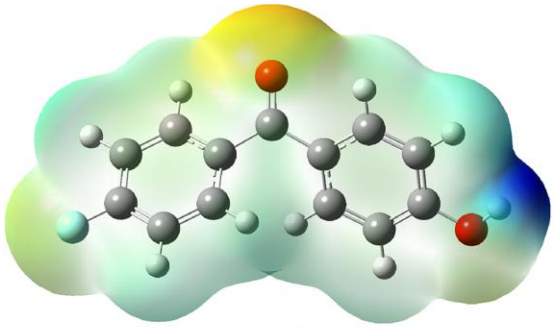

(a)

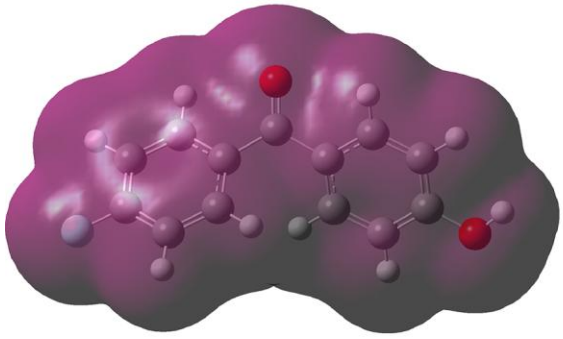

(b)

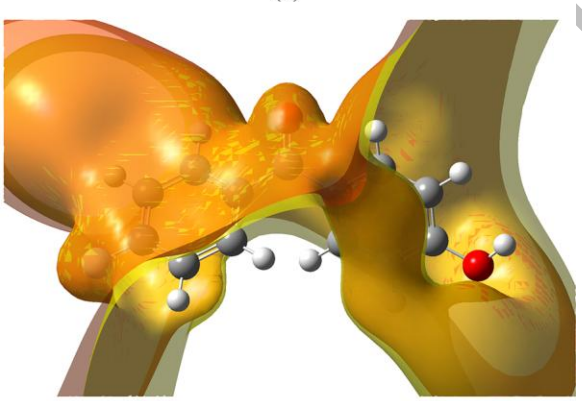

(c)

Accepted Manuscript

Figure 4. UV-visible absorption spectra of 4-fluoro-4-hydroxybenzophenone molecule in (a) gas phase; (b) dimethyl sulfoxide; (c) chloroform; (d) ethanol.

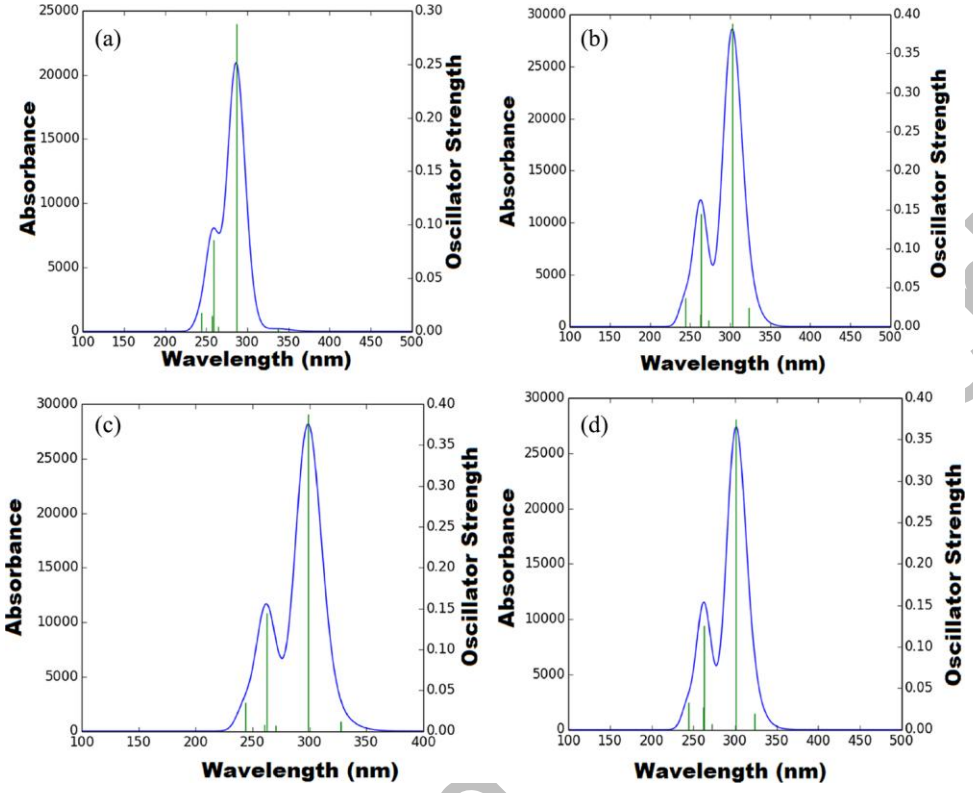

Accepted Manuscript

Figure 5. Experimental (top) and simulated (bottom) (a) Infrared spectra; (b) Raman spectra of 4-fluoro-4-hydroxybenzophenone molecule

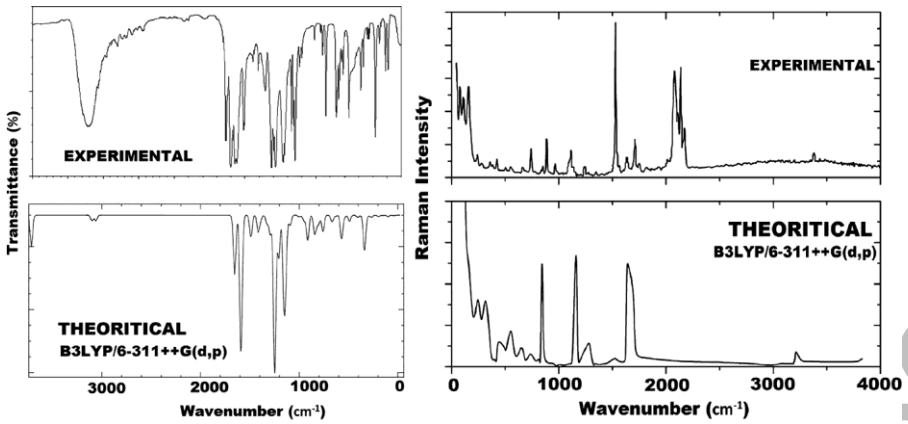

Accepted Manuscript